Preprints (www.preprints.org) | NOT PEER-REVIEWED | Posted: 25 July 2019 doi:10.20944/preprints201907.0281.v1

Article

Heat Pump Dryer Design Optimization Algorithm

Bernardo Andrade [1,3], Ighor Amorim [2,3], Michel Silva [2,3,6], Larysa Savosh [4], Luís Frölén Ribeiro [3,5,*]

[1] CEFET-MG – Brazil
[2] UTFPR – Ponta Grossa – Brazil
[3] Mechanical Technology Department - Polytechnic Institute of Bragança – Portugal
[4] Lutsk National Technical University – Ukraine
[5] Centre for Renewable Energy Research - INEGI – Portugal
[6] Team4cooling – Portugal

* Correspondence: frolen@ipb.pt; Tel.: +351-273303148 (L.F.R.)

Abstract: Drying food involves complex physical atmospheric mechanisms with non-linear relations from the air-food interactions. Moreover, those relations are strongly dependent on the moisture contents and the actual type of food. Such dependence makes it complex to design suitable machines dedicated to a single drying process. To speed-up and streamline the drying machine design, a heat pump dryer design optimization algorithm was developed. The proposed algorithm inputs food and air proprieties, the volume of the drying container and the technical specifications of the heat-pump off-the shelf components. The heat required to dehumidify the food equals the heat exchange process from condenser to evaporator, and the compressor's requirements (refrigerant mass flow rate and operating pressures) are then calculated. Compressors can then be select based in the volume and type of food to be dried. The algorithm is shown via a flow chart to guide the reader throughout 3 different stages representing each singular physical phenomenon: analysis of the internal air properties; heat flow analysis between components, air and food; food humidity calculus and verification. Results of the application of the algorithm are presented for the drying of *Agaricus Blazei* mushroom with 3 different humidity contents (60, 80 and 88% of water) for batches of about 45, 123, 200, 277 and 355 kilograms. The results indicate that for the first batch a 610 W compressor will suffice, while for the second one a 990 W compressor will deliver the required work to the refrigerant gas. Further, the last 3 ones would demand for a more potent 1445 W compressor.

Keywords: Algorithm; Heat-Pump; Drying; Food; Design; Optimization

1. Introduction

Food drying is one of the most energy consuming processes there exist, corresponding to about 10% to 25% of the total energy consumed in manufacturing installations. One type of these food preservation mechanisms is thermal based and is complex. It involves the removal of a solid product`s humidity by the employment of heat. The drying occurs through heat and mass transfers while the properties of the food change throughout the process. There are many different machines that can make this process, one of these is heat-pump based [1].

This machine extract energy via a gas compressor from a cold-source and delivers it to a hot-source. It does so by providing work to the refrigerant fluid. The heat-pump provides heat, making it directly useful for heating ventilation and air conditioning (HVAC), but also for drying applications. The machine energy input is the energy received from the compressor and adds it to the amount of energy removed from the cold-source, yielding a higher energy output. As an example, for a compressor yielding 100 W to remove 400 W from a cold-source, the total amount of energy provided to the hot-source will be 500 W. This is a 5-time higher value than the one extracted by the

Preprints (www.preprints.org) | NOT PEER-REVIEWED | Posted: 25 July 2019 doi:10.20944/preprints201907.0281.v1

compressor, meaning a 500 W heating service from a 100 W electrical input. This highlights the energy saving feature of this technology. A scheme of the whole machine and its components is shown in Fig 1: compressor, expansion valve and heat exchangers (condenser and evaporator).

The work cycle starts with the air being heated at the condenser after being blown towards the product (A to B in Fig.1). When the warm air passes by the food, it removes humidity from the material. Downstream, the air captured the moisture from the food (B to C in Fig.1). It then heads to the evaporator, to partially condense some of its water. This (C to A in Fig.1) is achieved by promoting the heat transfer of the air with colder dew-point surfaces of the evaporator.

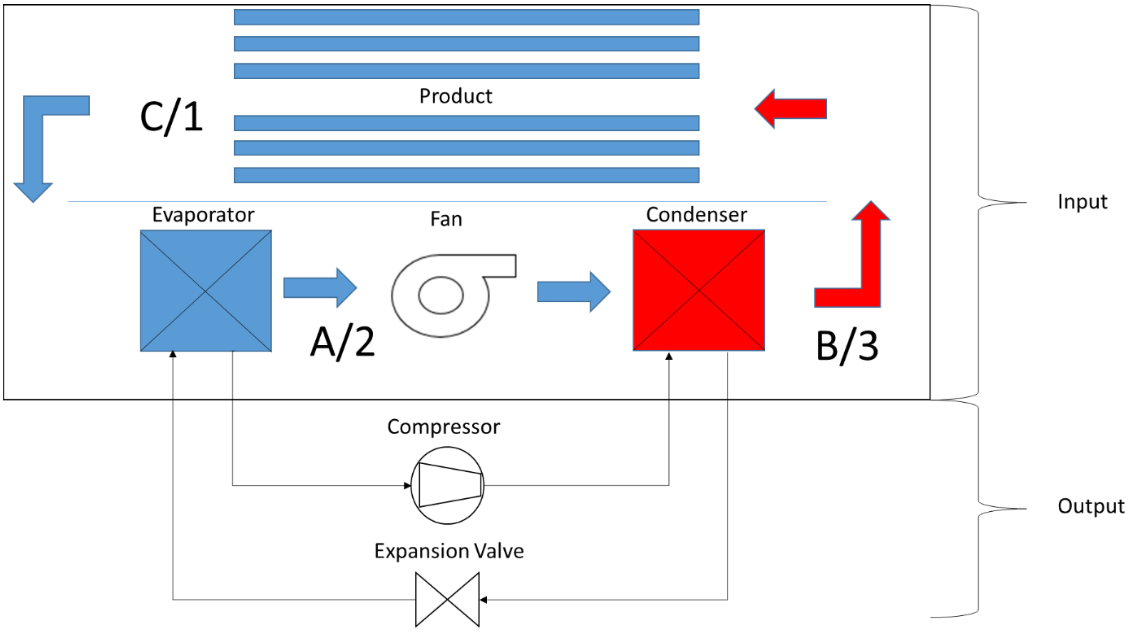

Figure 1. Scheme of heat pump for drying food. The thin line represents the refrigerant circuit while the thick arrows represent the air-flow circuit.

The design of this machine for different purposes, or types of food, can be improved by the application of resources such as the numerical optimization.

Improving equipment design takes time and laboratorial costs which are not directly translated towards the manufacturing process, for the material acquired is usually spent on tests. Mathematical models and computational mechanics are effective alternatives to many practical experiments since they provide a prediction of what may happen and what is to be expected. This approach allows for greater comprehension of the transport phenomena involved in the drying of food and improves the testing and production process control which leads to better designing [2].

A simulation can also have an edge on normal experiments for it can predict, with virtual sensors, the humidity, air velocity and temperature on points that are normally inaccessible since the presence of the sensors would impact the air circulation inside the drying container. Also, there is no limitation of testing different working conditions, there is no space restriction nor need for trained operators. However, simulations require reliable data and proper modelling, otherwise the quality of results may be questionable. This is true for the case of drying food especially describing the physical/chemical properties and transport phenomena.

To achieve better results in energy efficiency and product quality, studies have been performed on this area and new models of heat-pump dryers have been created [2,4]. And so, the use of algorithms comes into play as the driving force of better product design, enabling the creation of products directed to many markets: from food industry to the small-scale farmer.

An algorithm is proposed in this article to aid the selection of heat-pump components. It is presented through a flow chart that helps the designer visualize and comprehend the specified numerical solution`s steps. The article is concluded by an example of inputs and outputs of a code created from the algorithm and it is discussed how these results can help the development of different size drying machines.

2. Materials and Methods

The design algorithm is a logic map of efficient design of food-drying heat-pump air-based machines. The algorithm inputs are the type of food, the air properties and the dimensions of the food container, as well as the dryer component properties. To guarantee the temperature control throughout the drying process, the working temperature of the air to which the food is being exposed to is used as input. Therefore, it is possible to ascertain the final product quality, since over-heating could cause damage to the product. Meanwhile, the algorithm outputs the mass flow of refrigerant fluid from which the compressor and expansion valve can be selected. The difference of the algorithm inputs and outputs, and their relation to the machine design are depicted in Fig.1. In this figure within the circulating air volume there are 2 different nomenclatures aiming the description of different things: A, B and C that are related only to the air proprieties; 1, 2 and 3 that represents the 3 stages of the algorithm, with the different transport and energy equations.

1. Internal air analysis;
2. Heat flow analysis between components, air and food / component design;
3. Food humidity calculus and verification.

2.1. Stage 1 of the algorithm

The first stage of the algorithm determines the psychrometric and dynamic states of the air. The literature recommends temperatures for drying each food, and by using them in the following psychrometric and transport equations, one obtains every property necessary to the characterization of the process and posterior steps [5–7].

The calculus of the air properties are given by Eq. (1) to (17) while the specific psychometry Eq. (1-8) are recommended by [6]. The psychrometric equations utilized at this stage describe the humid air based on its temperature, amount of water as vapor and the air`s occupied volume [8–10].

To provide the readers less clutter information on the variables of the equations, a list of variables and units is shown in the end of the article.

At first it is necessary to obtain the vapor saturation pressure P_{vs} and the absolute humidity w. The air humidity after the contact with the food in the first iteration and after the air leaves the evaporator, corresponding to air process C and A in Fig. 1, are calculated by Eq. (1) and (2):

$$P_{vs} = 6\frac{10^{25}}{1000 * T^5} \cdot exp\left(-\frac{6800}{T}\right) \tag{1}$$

$$w = \frac{0.622\, P_v}{P_{atm} - P_v} \tag{2}$$

In the following iterations, the absolute humidity is obtained by adding the total humidity lost by the food to the air humidity after it left the condenser, process B to C in Fig. 1. The air humidity when it leaves the condenser is equal to the one when it left the evaporator. Therefore, the next step are the calculations of the air`s vapor pressure Pv, and its enthalpy H, from the absolute humidity Eq.(3) and Eq.(4):

$$P_v = w \cdot \frac{P_{atm}}{0.622 + 0.378 * w} \tag{3}$$

$$H = 1.006 \cdot (T - 273.15) + U_{ab}[2501 + 1.775 \cdot (T - 273.15)] \tag{4}$$

Preprints (www.preprints.org) | NOT PEER-REVIEWED | Posted: 25 July 2019 doi:10.20944/preprints201907.0281.v1

With the air`s vapor pressure and the vapor saturation pressure, the relative humidity $\emptyset$ and the dew point Tdp are then calculated for this pressure, Eq. (5) and (6).

$$\emptyset = \frac{P_v}{P_{vs}} \tag{5}$$

$$T_{dp} = \frac{186.4905 - 237.3 \log 10 \cdot P_v}{\log(10\, P_v) - 8.2859} \tag{6}$$

Also, with the vapor`s pressure and the absolute humidity, the algorithm calculates the specific volume v, vapor molar fraction X_v relative to the mixture and molar mass.

$$X_v = \frac{P_v}{P_{atm}} \tag{7}$$

$$v = 0.28705T \cdot \frac{1 + 1.6078w}{P_{atm}} \tag{8}$$

The determination of the transport properties require the following proportion non-dimensional parameters Φ_{av} and Φ_{va}, as recommended by [7] and presented in Eq. (9) and (10).

$$\Phi_{av} = \frac{\sqrt{2}}{4}\left(1 + \frac{M_a}{M_v}\right)^{-\frac{1}{2}}\left[1 + \left(\frac{\mu_a}{\mu_v}\right)^{\frac{1}{2}}\left(\frac{M_a}{M_v}\right)^{\frac{1}{4}}\right]^2 \tag{9}$$

$$\Phi_{va} = \frac{\sqrt{2}}{4}\left(1 + \frac{M_v}{M_a}\right)^{-\frac{1}{2}}\left[1 + \left(\frac{\mu_v}{\mu_a}\right)^{\frac{1}{2}}\left(\frac{M_a}{M_v}\right)^{\frac{1}{4}}\right]^2 \tag{10}$$

The acronyms M_v and M_a respectively represent the molar masses of the vapor and dry air while the μ_v and μ_a represent their dynamic viscosity. Therefore, with the proportion parameters Φ_{av} and Φ_{va} defined, the mean thermophysical properties are calculated.

Firstly, the thermal conductivity of the humid air k_{ar} is given by Eq. (11).

$$k_{ar} = \frac{(1 - x_v)k_a}{(1 - x_v) + x_v\Phi_{av}} + \frac{x_v k_v}{x_v + (1 - x_v)\Phi_{av}} \tag{11}$$

And, the specific heat cp_m of this air is obtained with Eq. (12).

$$cp_m = cp_a x_a \frac{M_a}{M_m} + cp_v x_v \frac{M_v}{M_m} \tag{12}$$

These properties are used to obtain the thermal diffusivity α, which is expressed by Eq. (13).

$$\alpha = \frac{k}{\rho * c_{pm}} \tag{13}$$

Also, the mixture density ρ for incompressible gases are calculated according to Eq. (14):

$$\rho = \frac{P_0}{RT}\left[1 - x_v\left(1 - \frac{M_v}{a}\right)\right] \tag{14}$$

The transport properties that govern the fluid`s movement are calculated from the equations pointed by [7]. The dynamic viscosity μ_{mix}, of the mixture results from Eq. (15):

$$\mu_{mix} = \frac{(1 - x_v)\mu_{ar}}{(1 - x_v) + x_v\Phi_{av}} + \frac{x_v\mu_{vapor}}{(1 - x_v) + x_v\Phi_{va}} \tag{15}$$

With μ_{mix} and ρ, the cinematic viscosity τ then is obtained with Eq. (16):

Preprints (www.preprints.org) | NOT PEER-REVIEWED | Posted: 25 July 2019 doi:10.20944/preprints201907.0281.v1

$$\tau = \frac{\mu_{mix}}{\rho} \tag{16}$$

The Prandl number Pr, which is used to determine the water loss, is calculated from Eq. (17):

$$Pr = \mu_{mix}\frac{cp_m}{k} \tag{17}$$

2.2. Stage 2 of the algorithm

The second stage of the algorithm related to the heat flow analysis and component design, uses the data calculated in Stage 1, the pre-determined dimensions and construction parameters of components to calculate results that are essential to the final design of the product.

However, the creation of something novel from scratch is very costly so the algorithm uses as entry data for the second stage: the operation temperatures and the catalogued dimensions of off-the-shelf products of both heat exchangers and fans. Because a heat-pump system can be defined by the compressor and the heat exchangers [9], the heat output of this stage will be used on calculating the mass flow rate of refrigerant required to select a fitting compressor.

The reasoning behind this is that controlled temperatures are a main focus of the algorithm, to assure product quality. Also, the heat exchangers and fans are parts that affect the final product dimension if changed, and so, by selecting products that are available in the market, the cost of production is expected to drop and the final product construction can be streamlined. Any machine designed through this method will have its power output controlled through the variation of the compressor`s cycle rate.

At this stage the fans diameter is used with previously calculated air speed and density to obtain the air mass flow rate, which will be used in the third stage for controlling the removed water.

With the combined data from Stage 1 and the dimensions of components, the heat which will flow to the air is calculated. That heat is the same that is removed from the refrigerant fluid, and since the temperatures have been set, the enthalpy variation of the refrigerant expected is known and so its mass flow rate is achieved.

To do so, the equations used were the ones that relate to the heat exchangers, such as logarithmic mean temperature difference, Nusselt and Reynolds dimensionless numbers, global heat conductivity and heat flow equation at heat exchangers. These equations are pointed out in [12–15].

The logarithmic mean temperature difference ΔT_{ml} is a variable that accounts for the logarithmic nature of the heat transfer properties and converts the temperatures and the exchanger`s entry and exit, jointly with the external`s fluid temperature to obtain a mean value that can be used in heat transfer equations.

$$\Delta T_{ml} = \frac{(T_{med} - T_{ent}) - (T_{med} - T_{sai})}{\log\frac{(T_{med} - T_{ent})}{(T_{med} - T_{sai})}} \tag{18}$$

These equations also require a mean global heat flux coefficient U. This has the same principle of the previous Eq. (18), making a mean value that accounts for every heat transfer process. However, unlike the logarithmic mean temperature difference, this equation results in a heat transfer factor.

$$\dot{U} = \frac{1}{\frac{1}{h} + \frac{l}{k}} \tag{19}$$

Where l represents the thickness of the heat exchanger's walls.

And so, the required data to calculate such a factor are the conduction heat transfer coefficient for the heat exchanger`s material k, and the convection heat transfer coefficient for the operating air flow h.

Preprints (www.preprints.org) | NOT PEER-REVIEWED | Posted: 25 July 2019 doi:10.20944/preprints201907.0281.v1

$$h = \mathrm{k}_{ar}\frac{Nu}{D} \tag{20}$$

Where D equals to the heat exchanger`s cylinder diameter $\mathrm{k}_{ar}$ is the air`s heat conductivity and Nu is a dimensionless number obtained through the following equation:

$$Nu = 1.13\, Re^{M} \cdot C \cdot Pr \tag{21}$$

In this equation, the M and C variables are constants obtained based on the heat exchanger`s dimensions and layout. The Re is another number obtained by:

$$Re = \frac{\rho V D}{\mu} \tag{22}$$

The V in the equation is the air`s speed. Finally, the final exchanged heat value $\dot{Q}$, equals to:

$$\dot{Q} = \dot{U} A \Delta T_{ml} \tag{23}$$

Where A is the total exposed heat exchanger area. The heat can be used, as previously mentioned, together with the variation of enthalpy ΔH , to obtain the refrigerant mass flow rate $\dot{m}$.

$$\dot{m} = \frac{\dot{Q}}{\Delta H} \tag{24}$$

2.3. Stage 3 of the algorithm

The third stage, the food analysis, is a control stage. This means that in it the algorithm has its control variables calculated to provide the iterative results that make the calculating cycles continue or stop. For this case, the control variable is food`s humidity level, and it is calculated through the use of well-known food-drying models. The Modified Henderson model was selected for its recurring appearance in the literature and consequent versatility. It requires the air`s humidity level, temperature and speed to calculate the water loss variation [4, 5].

For the calculus of the water mass transfer and consequently total humidity left in the product, the air diffusion coefficient is cited at [12, 16]:

$$D_{ab} = 1.87 \times 10^{-10}\frac{T^{2.072}}{P} \tag{25}$$

With this value, the Graschof Gr and Schimdt Sc numbers can be obtained:

$$Gr = \frac{g \Delta \rho S^{3}}{\rho \tau^{2}} \tag{26}$$

$$Sc = \frac{\tau}{D_{ab}} \tag{27}$$

Where Sc is the characteristic dimension, which in the case of the drying machine are the spaces between the plaques that hold the food. With both Graschof and Schimdt, the Rayleigh Ra and Sherwood numbers can be obtained, for both natural Sh_n and forced Sh_f convections:

$$Ra = Gr \cdot Sc \tag{28}$$

$$Sh_n = 0.197\left(Ra^{\frac{1}{4}}\left(\frac{hp}{S}\right)^{\frac{1}{9}}\right) \tag{29}$$

If Reynolds is inferior to 200.000,

Preprints (www.preprints.org) | NOT PEER-REVIEWED | Posted: 25 July 2019 doi:10.20944/preprints201907.0281.v1

$$Sh_f = 0.664(Re^{0.5} * Sc^{\frac{1}{3}}) \tag{30}$$

But for a superior value,

$$Sh_f = 0.0365(Re^{0.8} * Sc^{\frac{1}{3}}) \tag{31}$$

With Sherwood defined, the mass transfer coefficient is obtained with Eq. (32).

$$hcf = Sh\frac{D_{ab}}{hp} \tag{32}$$

The hp value is the food containing plaque`s height. The total water mass removed m_l is calculated by:

$$m_l = hcf \cdot ns \cdot Ap \cdot \Delta\rho \tag{33}$$

In Eq. (33), Ap is the plaque`s area, ns is the number of plaques and $\Delta\rho$ is the difference between density of water in the air and food.

The next step of the algorithm compares the value obtained with the mass transfer equation and the Modified Henderson model, and select the most conservative value. This value is removed from the food`s total humidity and accounted for in the control function, restarting the cycle if necessary.

3. Results

The algorithm can be represented in the form of a flow chart, to illustrate the proposed logic map. The first stage shown in Fig.2 results in the definition of the air`s psychrometric and transport properties throughout the drying process, doing so from the Eq. (1) to (17) and the input data both from the food and from the machine.

Preprints (www.preprints.org) | NOT PEER-REVIEWED | Posted: 25 July 2019 doi:10.20944/preprints201907.0281.v1

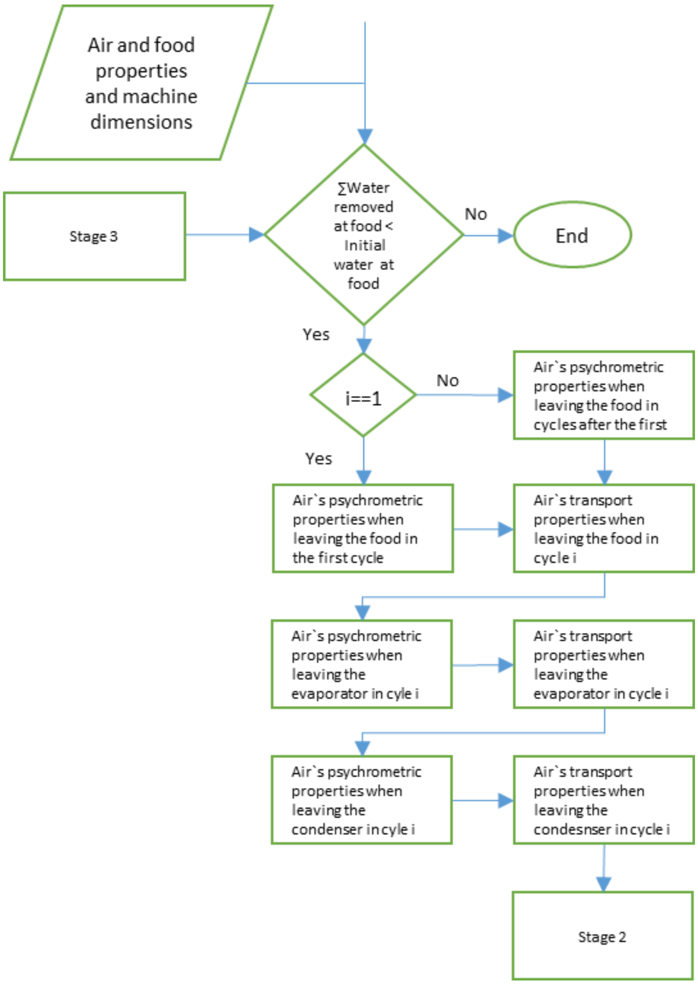

Figure 2. Stage 1 of the algorithm. The internal air analysis described in Eq. (1) to (17).

The properties outputs are used mainly as input for other stages. However, the program still can provide this data to guarantee quality control, specifically through the monitoring of the air`s temperature at the exit of each component.

The second stage shown in Fig.3 outputs both design and process parameters. By taking the aforementioned properties, it calculates the heat required to change the air`s state at both condenser and evaporator. With it, and the expected enthalpy variation, the refrigerant mass flow rate is achieved. These characteristics allow for an easy selection of the components required to design the heat-pump of the dryer. These components are: compressor, expansion- valve, refrigerant fluid and heat exchangers.

Even though the algorithm allows for easier selection of components, there still are some parts that require manual selection. As commented in Section 2, the fans that circulate the air are pre-selected to fit the drying container so that their dimensions are used as input data to calculate the mass flow rate of the circulating air inside the machine.

Preprints (www.preprints.org) | NOT PEER-REVIEWED | Posted: 25 July 2019 doi:10.20944/preprints201907.0281.v1

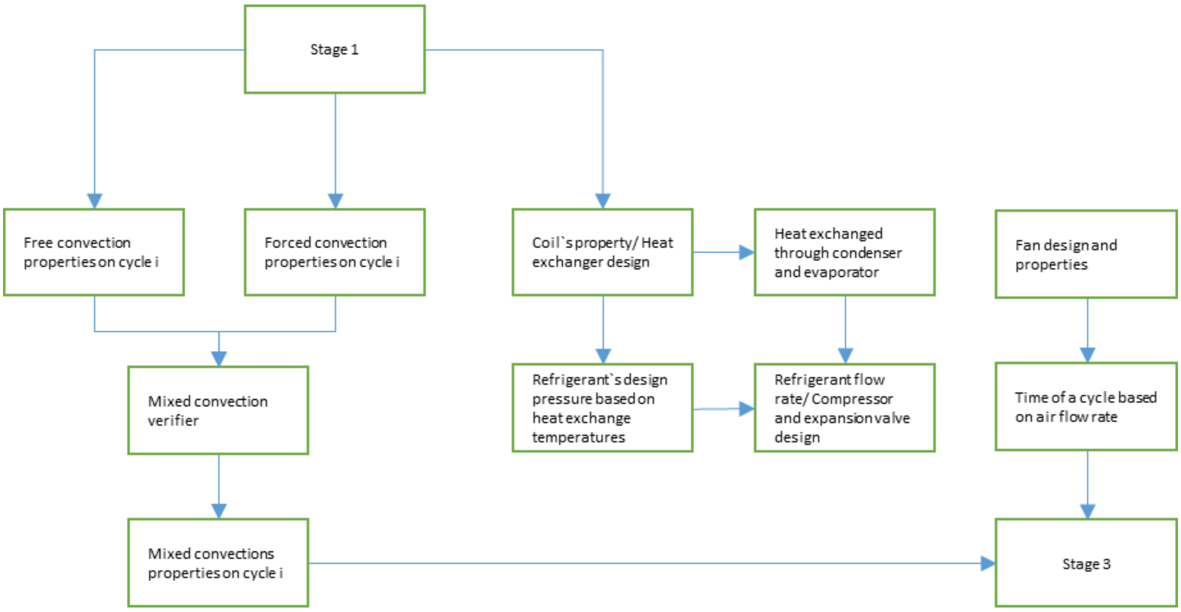

Figure 3. Stage 2 of algorithm. Heat flow analysis between components, air and food. Component design derived from Eq. (18) to (24).

For the final stage shown in Fig. 4, the results are given as a function of the amount of water in the system. The algorithm outputs the rate of water removal. From it, the algorithm calculates how this rate varies and how it effects the drying food. Finally, the variation of how much water is being removed is used as a parameter for cycle control and break function.

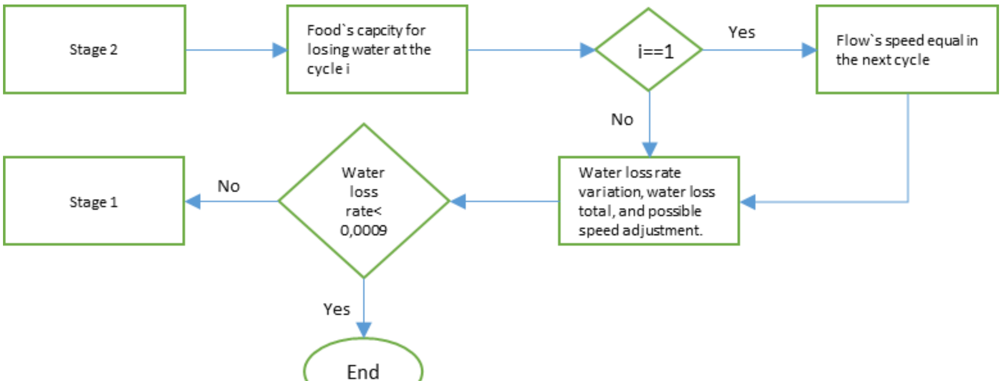

Figure 4. Stage 3 of algorithm. Food humidity calculus and verification as demonstrated from Eq. (25) to (33).

The whole algorithm is depicted in Fig. 5 showing the 3 stages that correspond, in Fig. 1, to the A-B, B-C and C-A thermal processes.

Preprints (www.preprints.org) | NOT PEER-REVIEWED | Posted: 25 July 2019 doi:10.20944/preprints201907.0281.v1

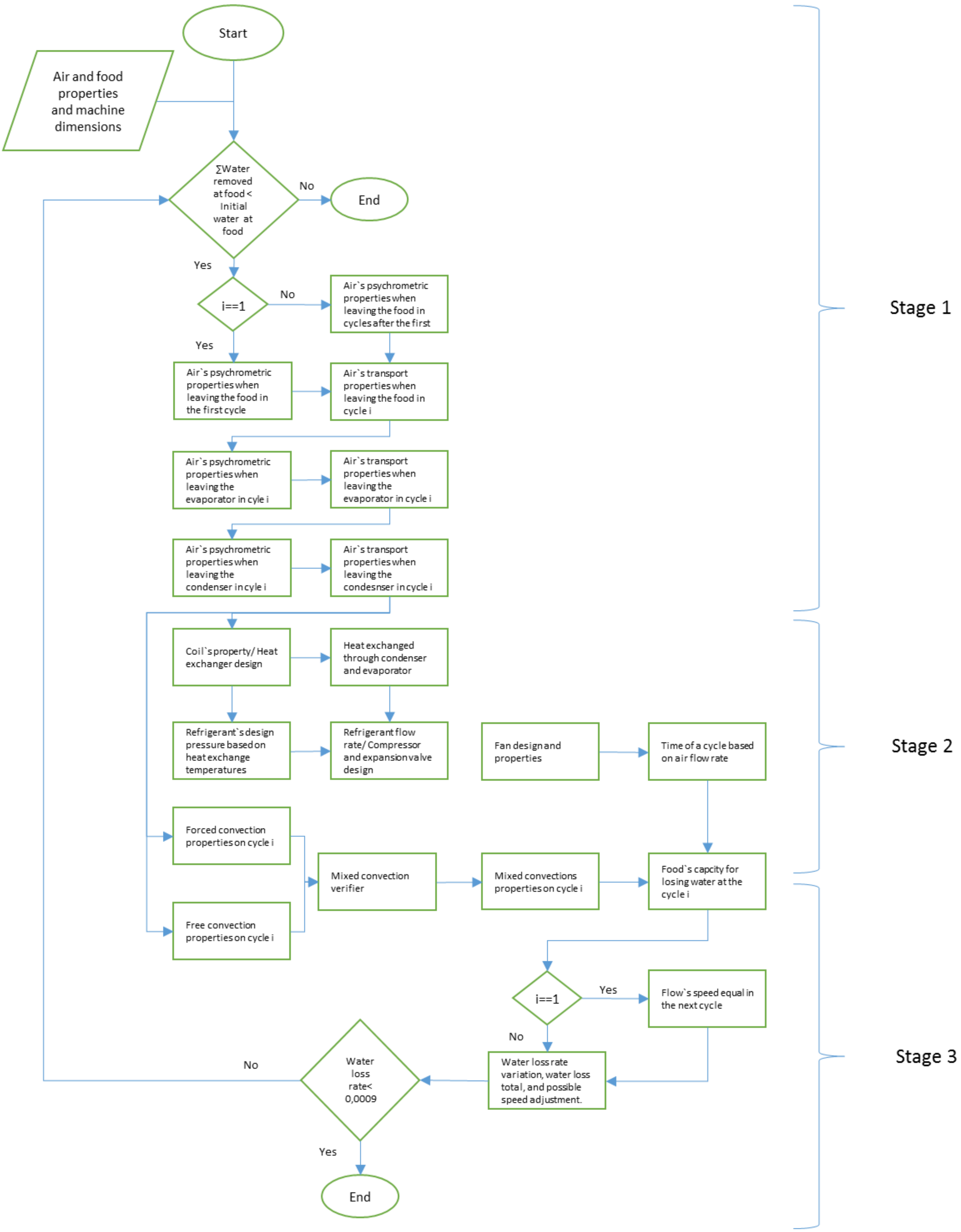

Figure 5. Heat pump dryer design optimization algorithm

 doi:10.20944/preprints201907.0281.v1

4. Discussion

The flow chart allows for an easier overview of the process (Fig. 5). This handy resource guides its user from a basic starting point towards its desired goal which makes designing simpler, since every information required can be traced back to information available in the market.

The proposed algorithm is a tool of how to design the heat-pump air-based drier being also a step-by-step guide. Though it may be also used to write a program that will automate the calculations, it is not restricted by the physical models hereby proposed. This is a strong characteristic of the algorithm because it is possible to update the used models of each process to the newest and most sound ones available. Doing so, and using more accurate data will impact on the precision of the final result. Actually, such a practice was used in the development of this algorithm. Data and equations found in earlier versions of established guides and books such as [8] and [10] were posteriorly replaced by newer ones [7].

The algorithm specifies each step and allows for the comprehension of the necessary and produced data for that step. Meanwhile, a simulation program takes every step and automates, making the calculation sequence so that it will output a final value, and not clutter the user with processual information.

In order to exemplify the application of the proposed algorithm, a code written in GNU Octave simulated the drying of the *Agaricus Blazei* mushroom for batches of varying volumes that correspond to about 45, 123, 200, 277 and 355 kilograms of product. To simulate the drying, and consequently provide suitable data for the design, it was considered the properties pointed out by [5] related to the product`s fraction of water. Also, the input for stage two related to the heat-exchangers and fan dimensions were based on the ECO coils and coolers of the Luvata Company.

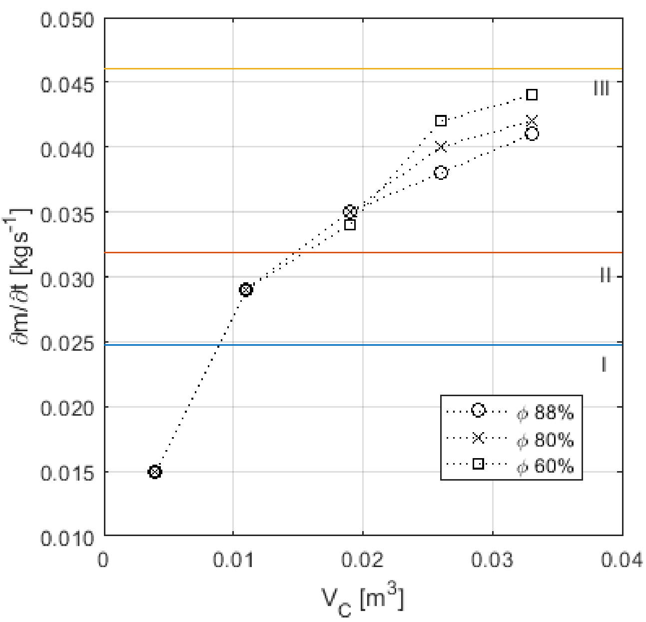

Figure 6. Relation of volume of product to required refrigerant flow.

Considering that 90% of the drying container`s volume is filled with food and that the mushroom`s amount of water for 3 different cases is: 60%, 80% and 88%, the humidity removed can be calculated based on the container's volume. This is used to create a variable parameter from which the power output can be measured. Also, the temperature of drying was set to 80 °C, the superior temperature limit from which this particular mushroom species starts having chemical and organoleptic changes.

The algorithm simulated humidity removal for those given conditions and the results are depicted in Fig. 6. The refrigerant mass flow rate is plotted against the volume of food in the drying container, being a critical information for the selection of a suitable compressor. A commercial compressor for nominal power operations yields a maximum mass flow rate. The graph represents

doi:10.20944/preprints201907.0281.v1

these working limits of 3 types of compressors from a given manufacturer (EMBRACO). The number I, II and III respectively represent increasingly potent compressors of 610, 990 and 1445 W.

The simulation results show a clear need to upgrade the compressor from type I to II while increasing the amount of *Agaricus Blazei* mushrooms from 45 to 123 kg, a 2.73-fold increase in drying needs to a 1.6 increase in compressor power. Furthermore, an increase of 1.6 times, from 123 to 200 kg, will require a power increase of 1.46 times. The non-linearity of the drying process is clear, and in this example, for the larger batches, from 200 to 355 kg, only one type of compressor would suffice.

For smaller batches the amount of humidity in the food is negligible for design purposes, however for larger batches the power needs are quite different. The dryer the food is, the harder the compressor will have to work as it is depicted in Fig. 6. This is a known result and good indication of the proper response of the algorithm.

For further research the authors recommend that future versions of the algorithm, and possible programs, incorporate the use of fuzzy logic in its solving methodology. This is due to the logarithmic nature of both heat and mass transfer processes which make the use of a break function essential as indicated in Fig. 4 related to the end process of Stage 3. Fuzzy logic would make the idea of an ideal stopping point much more graspable and closer to reality.

5. Conclusions

A flexible optimization algorithm is presented, aimed to help heat-pump air-based dryers design incorporating off-the-shelf components. The algorithm is segmented into 3 parts allowing the modification or upgrade of any one according to new scientific developments. It also allows dedicated solutions for different types and quantities of food because it incorporates their own chemical and organoleptic limitations.

With this guide in hand, the selection of components and materials is simpler because the users will have the key parameters of the required components and streamline the iterative process of machine design.

Appendix A

List of variables and units.

P_{vs}	Vapor saturation pressure	[pa]
w	Absolute humidity	[kg water/kg air]
Pv	Air`s vapor pressure	[pa]
H	Enthalpy	[kJ/kg*K]
$\emptyset$	Relative humidity	
Tdp	Dew point	[K]
v	Specific volume	[m³/kg]
X_v	Vapor molar fraction	
k_{ar}	Thermal conductivity of the humid air	[W/m²*K]
cp_m	Specific heat	[kJ/kg*K]
α	Thermal diffusivity	[m²/s]
ρ	Mixture density	[kg/m³]
μ_{mix}	Dynamic viscosity	[N*s/m²]
τ	Kinematic viscosity	[m²/s]
ΔT_{ml}	Logarithmic mean temperature difference	[K]
$\dot{U}$	Mean global heat flux coefficient	[W/m²*k]

l	Thickness of the heat exchanger's walls	[m]
k	Heat transfer coefficient of material	[W/m²*K]
h	Convection heat transfer coefficient	[W/m²*K]
V	Air`s speed	[m/s]
A	Total exposed heat exchanger area	[m²]
$\dot{m}$ or $\frac{\partial m}{\partial t}$	Mass flow rate	[kg/s]
D_{ab}	Air diffusion coefficient	[m²/s]
m_l	Total water mass removed	[kg/s]
Ap	Plaque`s area	[m²]

References

[1] M. Aktaş, L. Taşeri, S. Şevik, M. Gülcü, G. Uysal Seçkin, and E. C. Dolgun, “Heat pump drying of grape pomace: Performance and product quality analysis,” *Dry. Technol.*, vol. 0, no. 0, pp. 1–14, 2019.

[2] N. Malekjani and S. M. Jafari, “Simulation of food drying processes by Computational Fluid Dynamics (CFD); recent advances and approaches,” *Trends Food Sci. Technol.*, vol. 78, no. December 2017, pp. 206–223, 2018.

[3] Á. Castell-Palou and S. Simal, “Heat pump drying kinetics of a pressed type cheese,” *LWT - Food Sci. Technol.*, vol. 44, no. 2, pp. 489–494, 2011.

[4] V. Demir, T. Gunhan, and A. K. Yagcioglu, “Mathematical modelling of convection drying of green table olives,” *Biosyst. Eng.*, vol. 98, no. 1, pp. 47–53, 2007.

[5] L. E. Kurozowa, “Efeito das condições de processo na cinética de secagem de cogumelo,” p. 121, 2005.

[6] R. P. Lopes, D. C. Lopes, and R. C. Rezende, *Secagem e Armazenagem de Produtos Agrícolas*. Aprenda Fácil Editora ISBN 978-85-62032-00-4, 2008.

[7] P. T. Tsilingiris, “Thermophysical and transport properties of humid air at temperature range between 0 and 100 °C,” *Energy Convers. Manag.*, vol. 49, no. 5, pp. 1098–1110, 2008.

[8] A. S. of H. R. and A. C. Engineer, *2015 ASHRAE HANDBOOK Inch-Pound Edition*. 2015.

[9] N. Yamankaradeniz, K. F. Sokmen, S. Coskun, O. Kaynakli, and B. Pastakkaya, “Performance analysis of a re-circulating heat pump dryer,” *Therm. Sci.*, vol. 20, no. 1, pp. 267–277, 2016.

[10] F. P. Incropera and F. P. Incropera, *Fundamentals of heat and mass transfer.*, 6th ed. John Wiley, 2007.

[11] Y. A. M. A. B. Cengel, *Thermodynamcis, An Engineering Approach*, 8th ed. Mc Graw-Hill Interamericana, 2007.

[12] L. J. Goh, M. Y. Othman, S. Mat, H. Ruslan, and K. Sopian, “Review of heat pump systems for drying application,” *Renew. Sustain. Energy Rev.*, vol. 15, no. 9, pp. 4788–4796, 2011.

[13] C. O. Perera and M. S. Rahman, “Heat pump dehumidifier drying of food,” *Trends Food Sci. Technol.*, vol. 8, no. 3, pp. 75–79, 1997.

[14] M. T. . and M. E.A., “Gaseous Diffusion Coefficients,” *J. Phys. Chem.*, vol. 118, 1972.